J. Fluid Mech. (2002), *vol.* 467, *pp.* 259–268.
DOI: 10.1017/S0022112002001477 Printed in the United Kingdom

Nonlinear interaction of ice cover with shallow water waves in channels

By XUN XIA[1] AND HUNG TAO SHEN[2]

[1]Specialty Materials Division, Corning Inc., HP-CB-08, Corning, NY 14831, USA

[2]Department of Civil and Environmental Engineering, Clarkson University, Potsdam, NY 13699-5710 USA

(Received 5 November 2001 and in revised form 14 March 2002)

A nonlinear analysis of the interaction between a water wave and a floating ice cover in river channels is presented. The one-dimensional weakly nonlinear equation for shallow water wave propagation in a uniform channel with a floating ice cover is derived. The ice cover is assumed to be a thin uniform elastic plate. The weakly nonlinear equation is a fifth-order KdV equation. Analytical solutions of the nonlinear periodic wave equation are obtained. These solutions show that the shape, wavelength and celerity of the nonlinear waves depend on the wave amplitude. The wave celerity is slightly smaller than the open water wave celerity. The wavelength decreases as the wave amplitude increases. Based on these solutions the fracture of the ice cover is analysed. The spacing between transverse cracks varies form 50 m to a few hundred metres with the corresponding wave amplitude varying from 0.2 to 0.8 m, depending on the thickness and strength of the cover. These results agree well with limited field observations.

1. Introduction

The breakup of a river ice cover can generally be classified as a thermal breakup or a mechanical breakup. In a thermal breakup the ice cover deteriorates and melts in place with no significant movement. The physics of thermal breakup is well understood (Shen & Chiang 1984). Mechanical breakup of a river ice cover is due to the fragmentation of the floating cover by hydraulic and mechanical forces associated with changes in river discharge and water level. Mechanical breakups can be categorized into pre-frontal and frontal modes (Prowse & Demuth 1989). The pre-frontal modes include the formation of longitudinal shore cracks and the breakup of the ice cover into long sections of ice sheets (Beltaos 1990; Shulyakovskii 1972). No significant longitudinal movement of ice cover occurs during the pre-frontal modes. The frontal mode represents failure of the ice cover coincident with the surge wave during the last stage of the breakup. Closely spaced transverse cracks are formed under the influence of the wave, which often leads to cracking of ice sheets into individual floes followed by severe ice runs and ice jams. In the last ten years, significant progress has been made on the understanding of the dynamics of ice runs and ice jams (Shen, Su & Liu 2000; Shen, Liu & Chen 2001). However, since a clear understanding of the mechanics of river ice breakup is not available, predictions of breakup and the associated ice jams still cannot be made. The lack of understanding of the mechanics of river ice breakup is mainly due to the lack of understanding of

the formation of closely spaced transverse cracks under the action of river waves, which is the key to the occurrence of breakup ice runs.

Wave–ice interaction has been studied extensively by sea ice researchers (e.g. Squire *et al.* 1995; Wadhams 2000). These studies were mainly concerned with the interaction of water waves with ice floes and the attenuation of waves with distance into the ice pack. Each ice floe is considered as a floating raft. The water beneath the ice is assumed to satisfy the Laplace equation together with a linearized kinematic boundary condition at the mean water surface. Daly (1995) used a linear analysis to study the interaction between river waves and ice covers, and suggested the possibility of the formation of transverse cracks spaced at 10 m or less by waves in the gravity wave range with small wave amplitude. This phenomenon has not been observed in the field. Parkinson (1982) observed cracks spaced at 50 to 200 m apart formed across the ice cover during the passage of a flood wave in the Liard-Mackenzie River, and the broken ice front was moving at a speed approximately equal to that of the free-surface surge wave. Gerard *et al.* (1984) and Prowse (1986) made similar observations. In this paper, a nonlinear analysis of the interaction of a floating river ice cover with shallow water waves and the formation of closely spaced transverse cracks is presented.

2. Problem formulation

In an analysis of wave propagation in ice-covered channels Daly (1993) found two ranges of five bands of wave celerity in the wavenumber spectrum. In the range with longer wavelength, which is termed the quasi-open-channel range, the cover is floating on the water surface at hydrostatic equilibrium. In the ice-influenced range, the pressure underneath the cover deviates from hydrostatic, and effects of friction and bed slopes can be neglected. For one-dimensional unsteady flow in a wide, rectangular channel with a uniform ice cover, the following mass and momentum conservation equations can be used for analysing wave–ice interaction:

$$\frac{\partial d}{\partial t} + \frac{\partial (ud)}{\partial x} = 0, \tag{1}$$

$$\frac{\partial u}{\partial t} + u\frac{\partial u}{\partial x} + g\frac{\partial d}{\partial x} + \frac{1}{\rho}\frac{\partial P'}{\partial x} = 0, \tag{2}$$

in which, x, t are space and time coordinates; u is flow velocity; d is flow depth under the cover; g is acceleration due to gravity; ρ is water density; and P is pressure deviation from the hydrostatic pressure. The compressibility of water is not considered, since it is not important when the ice cover is separated from the banks after the formation of longitudinal cracks. The ice cover is assumed to be a thin homogeneous elastic plate. The equation of motion of the cover can be written as

$$\frac{EI}{1-v^2}\frac{\partial^4 d}{\partial x^4} + \rho_i \eta \frac{\partial^2 d}{\partial t^2} + N\frac{\partial^2 d}{\partial x^2} - P' = 0, \tag{3}$$

in which E is elastic modulus of ice; I is moment of inertia of the ice cover cross-section; v is Poisson's ratio; N is a constant compressive axial force per unit width along the cover; ρ_i is the ice density; and η is the ice cover thickness.

It is convenient to let $u = u_0 + u'$; $d = d_0 + d'$, where u_0 and d_0 are constants that correspond to uniform flow conditions. Equations (1) to (3) can then be written as

$$\frac{\partial d'}{\partial t} + u_0\frac{\partial d'}{\partial x} + d_0\frac{\partial u'}{\partial x} + \frac{\partial (u'd')}{\partial x} = 0, \tag{4}$$

$$\frac{\partial u'}{\partial t} + u_0\frac{\partial u'}{\partial x} + u'\frac{\partial u'}{\partial x} + g\frac{\partial d'}{\partial x} + \frac{1}{\rho}\frac{\partial P'}{\partial x} = 0, \tag{5}$$

$$\frac{EI}{1-v^2}\frac{\partial^4 d'}{\partial x^4} + \rho_i\eta\frac{\partial^2 d'}{\partial t^2} + N\frac{\partial^2 d'}{\partial x^2} - P' = 0. \tag{6}$$

By substituting (6) into (5) and introducing the coordinate transformation $x' = x - u_0 t$ and $t' = t$, these equations can be reduced to the following dimensionless equations:

$$\frac{\partial d^*}{\partial t^*} + \frac{\partial u^*}{\partial x^*} + \varepsilon\frac{\partial (u^* d^*)}{\partial x^*} = 0, \tag{7}$$

$$\frac{\partial u^*}{\partial t^*} + \frac{\partial d^*}{\partial x^*} + \varepsilon u^*\frac{\partial u^*}{\partial x^*} + \delta\frac{\partial^5 d^*}{\partial x^{*5}} + N_0\frac{\partial^3 d^*}{\partial x^{*3}} + \gamma\left(\frac{\partial^3 d^*}{\partial t^{*2}\partial x^*} - 2F_r\frac{\partial^3 d^*}{\partial t^2\partial x^{*2}} + F_r^2\frac{\partial^3 d^*}{\partial x^{*3}}\right) = 0, \tag{8}$$

in which the dimensionless variables and parameters are scaled by a horizontal length scale L_0, a vertical scale d_0, and the wave amplitude a as

$$F_r = \frac{u_0}{\sqrt{g d_0}}; \quad \varepsilon = \frac{a}{d_0}; \quad \delta = \frac{EI}{(1-v^2)\rho g L_0^4} = \frac{l^4}{L_0^4}; \quad \gamma = \frac{\rho_i}{\rho}\frac{d_0\eta}{L_0^2}; \quad N_0 = \frac{N}{\rho g L_0^2} \tag{9a}$$

and

$$x^* = \frac{x'}{L_0}; \quad d^* = \frac{d'}{a}; \quad t^* = \frac{ct'}{L_0}; \quad u^* = \frac{d_0 u'}{ac}, \tag{9b}$$

in which the characteristic length of the cover

$$l = \left(\frac{EI}{\rho g(1-v^2)}\right)^{1/4} = \left(\frac{\eta^3 E}{12\rho g(1-v^2)}\right)^{1/4},$$

and $c = \sqrt{g d_0}$. Equations (7) and (8) are similar to the well-known Boussinesq equations (Debnath 1994; Mei 1983), albeit more complicated. Daly's (1995) linear analysis showed that waves with a wavelength of $2\pi l$ and amplitude of $O(0.1\,\mathrm{m})$ could cause transverse cracks to form. In such a case, the order of the ice stiffness parameter $\delta = (l/L_0)^4 = (1/2\pi)^4$ is 0.001, and the order of the small-amplitude parameter ε is 0.01 or larger. The nonlinear terms in (7) and (8) are comparable to the ice stiffness term, and could not be neglected. The linear analysis is therefore not valid.

3. Nonlinear analysis

Consider a solution of (7) and (8) correct to the first order in ε and δ in the form

$$u^* = d^* + \varepsilon Q_1 + \delta Q_2 + O(\varepsilon^2 + \delta^2), \tag{10}$$

where Q_1 and Q_2 are functions of d^* and its derivatives. The following equations for d^* and u^* can be obtained:

$$d^*_{t^*} + d^*_{x^*} + \frac{3}{2}\varepsilon d^* d^*_{x^*} + \frac{\delta}{2}d^*_{x^*x^*x^*x^*x^*} + \frac{\gamma}{2}(1+F_r)^2 d^*_{x^*x^*x^*} + \frac{N_0}{2}d^*_{x^*x^*x^*} + O(\varepsilon^2 + \varepsilon\delta + \delta^2) = 0, \tag{11}$$

$$u^* = d^* + \varepsilon\left(-\frac{d^{*2}}{4}\right) + \delta\frac{P^*}{2} + O(\varepsilon^2 + \varepsilon\delta + \delta^2), \tag{12}$$

where

$$P^* = \frac{\partial^4 d^*}{\partial x^{*4}} + \frac{\gamma}{\delta}\left(\frac{\partial^2 d^*}{\partial t^{*2}} - 2F_r\frac{\partial^2 d^*}{\partial x^*\partial t^*} + F_r^2\frac{\partial^2 d^*}{\partial x^{*2}}\right) + \frac{N_0}{\delta}\frac{\partial^2 d^*}{\partial x^{*2}}.$$

By dropping the prime in (9*b*) and neglecting terms of order ε^2, $\varepsilon\delta$ and δ^2, or higher, (11) in dimensional form becomes

$$\frac{1}{c}d_t + d_x + \frac{3}{2d_0}dd_x + \frac{l^4}{2}d_{xxxxx} + \frac{\rho_i}{2\rho}d_0\eta(1+F_r)^2 d_{xxx} + \frac{N}{2\rho g}d_{xxx} = 0. \tag{13}$$

The first two terms, $d_t + cd_x$, describe the wave evolution at the shallow-water wave speed. The third term with coefficient $3c/2d_0$ represents a nonlinear wave steepening. The rest of the terms are dispersion terms due to ice cover bending, inertia of the ice cover, and the axial force. Thus, (13) is a balance between time evolution, nonlinearity and dispersion. Equation (13), is a fifth-order Korteweg–de Vries equation, in the same form as the equation for weakly non-local solitary water waves (Grimshaw & Joshi 1995; Hunter & Scheurle 1988; Karpman 1998). However, in (13), the third-order terms are smaller than the fifth-order terms, i.e. ice cover bending dominates over the inertial and axial force terms.

We now seek a steady progressive wave solution of (13) travelling downstream. In the reference frame ζ so that $d = d(\zeta)$, $\zeta = x - Ut$, equation (13) gives the following equation after integration with respect to ζ:

$$A + \left(1 - \frac{U}{c}\right)d + \frac{3}{4d_0}d^2 + \frac{1}{2}d'''' + \beta d'' = 0, \tag{14}$$

in which

$$d' = \frac{d(d)}{d\xi}, \quad \xi = \frac{\zeta}{l} = \frac{x - Ut}{l}, \quad \beta = \frac{\rho_i}{2\rho}\frac{d_0\eta}{l^2}(1+F_r)^2 + \frac{N}{2\rho g l^2},$$

and A is an integration constant. The solution of (14) with negligible cover inertia and axial force is available from the authors or the Journal of Fluid Mechanics Editorial office.

3.1. *Solutions*

By neglecting the ice cover inertia and axial force terms in (14) the following explicit solution can be obtained:

$$d(x,t) = a\left(\frac{1}{3} - \mathrm{cn}^4\left(\left(\frac{a}{140d_0}\right)^{1/4}\frac{(x-Ut)}{l}, \sqrt{\frac{1}{2}}\right)\right), \tag{15}$$

and the wave speed U and wavelength L_w are

$$U = \left(1 - \frac{1}{10}\frac{a}{d_0}\right)c, \tag{16}$$

$$L_w = 2l\left(\frac{140d_0}{a}\right)^{1/4} K\left(\sqrt{\frac{1}{2}}\right), \tag{17}$$

where cn is the Jacobian elliptic function, and K is the complete elliptic integral of the first kind. Figure 1 shows the variation of the wave profile as given by (15). Equation (16) shows that the wave speed is slightly reduced from the shallow water wave speed in open channels, which is consistent with the field observations of Parkinson (1982). Equations (16) and (17) show that both the wave speed and wavelength decrease as the wave amplitude increases.

A cnoidal wave solution in the following form can be obtained for the complete

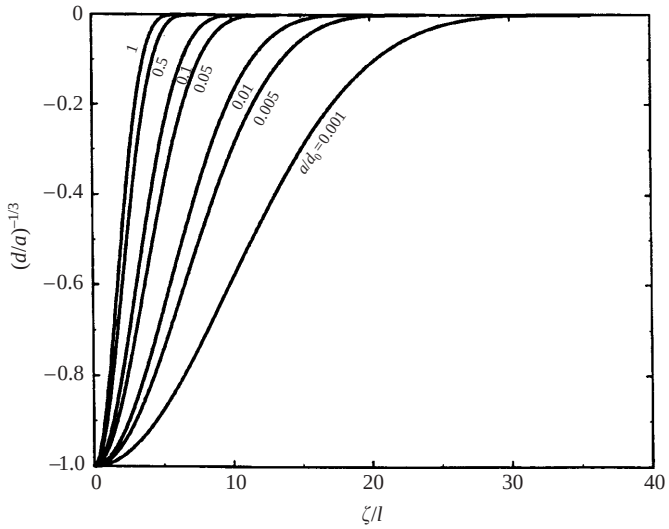

FIGURE 1. Dimensionless wave profile under ice cover for the first half-wavelength.

equation (14):

$$d(\zeta) = -a\,\mathrm{cn}^4\left(\alpha\frac{x-Ut}{l},\kappa\right) + b\,\mathrm{cn}^2\left(\alpha\frac{x-Ut}{l},\kappa\right) + g, \tag{18}$$

where a, b, g, α, κ, and U are given by the following five equations:

$$\frac{a}{d_0} = 560\kappa^4\alpha^4, \tag{19a}$$

$$\frac{b}{d_0} = -\left(\frac{14\times 80}{3}(1-2\kappa^2)\alpha^2 - \frac{14\times 40}{13\times 3}\beta\right)\kappa^2\alpha^2, \tag{19b}$$

$$\frac{g}{a} = \frac{-1}{39\kappa^2\frac{\alpha^2}{\beta}}\left(\frac{E(\kappa)}{K(\kappa)\kappa^2} - \frac{1-\kappa^2}{\kappa^2}\right) + \frac{1-\kappa^2}{3\kappa^2}, \tag{19c}$$

$$\frac{U}{c} = 1 + \frac{3a}{2d_0}\frac{g}{a} + Q, \tag{19d}$$

$$C_3\left(\frac{\alpha^2}{\beta}\right)^3 + C_2\left(\frac{\alpha^2}{\beta}\right)^2 + C_1\left(\frac{\alpha^2}{\beta}\right) + C_0 = 0, \tag{19e}$$

in which

$$Q = \left(16(53\kappa^4 - 53\kappa^2 + 8) + \left(40 - \frac{70\times 8}{3}\right)(1-2\kappa^2)^2\right)\alpha^4$$
$$+ \left(-20 + \frac{500}{3\times 13}\right)(-2\kappa^2+1)\beta\alpha^2 - \frac{2\times 31}{3\times 13^2}\beta^2, \tag{20a}$$

$$C_0 = -\frac{2\times 31}{3\times 13^2}, \tag{20b}$$

β	a (m)	b (m)	k	α	g	$U/c-1$
0.0079	0.323	0.01134	0.7126	0.16524	0.3164	−0.01146
0.0130	0.340	0.0192	0.7160	0.16660	0.3062	−0.01245
0.3130	0.330	0.2362	0.8382	0.18593	0.00047	−0.0678

TABLE 1. Solution of the complete equation for $L_w = 381.7$ m.

$$C_1 = \left[\frac{4}{13} + \left(-20 + \frac{500}{3\times 13}\right)\frac{1}{13} + \frac{4\times 31}{3\times 13^2}\right](-2\kappa^2+1), \tag{20c}$$

$$C_2 = 3\kappa^2 12(1-\kappa^2) - \frac{4}{13}(17\kappa^4 - 17\kappa^2 + 2) - 8(-2\kappa^2+1)^2$$
$$-2\left(-20 + \frac{500}{3\times 13}\right)(-2\kappa^2+1)^2$$
$$+\left(16(53\kappa^4 - 53\kappa^2 + 8) + \left(40 - \frac{70\times 8}{3}\right)(1-\kappa^2)^2\right)\Big/13, \tag{20d}$$

$$C_3 = 3\times 120(-2\kappa^4 + 3\kappa^2 - 1)\kappa^2 + 8(17\kappa^4 - 17\kappa^2 + 2)(-2\kappa^2+1)$$
$$-2(-2\kappa^2+1)\left(16(53\kappa^4 - 53\kappa^2 + 8) + \left(40 - \frac{70\times 8}{3}\right)(1-2\kappa^2)^2\right), \tag{20e}$$

where $E(\kappa)$ is the complete elliptic integral of the second kind; κ is the modulus of the elliptic function, which varies between 1 and 0; and U is the wave speed. The wave amplitude is determined by a and b. The wavelength L_w is calculated from

$$\frac{L_w}{l} = \frac{2}{\alpha}K(\kappa). \tag{21}$$

It is of interest to note that when $\kappa \to 0$, α approaches a constant, and both a and $b \to 0$. The solution approaches that of linear theory. When $\kappa \to \sqrt{\frac{1}{2}}$, both a and b approach positive infinity, and the solution for the complete equation approaches that of the simplified equation. Using a case with wavelength $L_w = 381.7$ m, $F_r = 0.3$, $d_0 = 3$ m, $E = 10$ GPa, and $\eta = 1$ m as an example, the solution of the complete equation is shown in table 1 for different values of β. Figure 2 shows the profiles of these nonlinear waves. The case with $\beta = 0$ in figure 2 corresponds to the solution of the simplified equation. Figure 2 also shows that when only ice inertia is considered, i.e. the case with $\beta = 0.0079$, the completed solution is almost identical to the simplified solution.

3.2. *Ice cover fracture*

The maximum bending stress in the ice cover occurs at the top or bottom, i.e.

$$S_{X\,max} = \frac{E}{1-\nu^2}\frac{\eta}{2}\frac{\partial^2 d}{\partial x^2}.$$

d_o (m)	E (Gpa)	η (m)	l (m)	a_{min} (m)	U (m s^{-1})	$L_{w\,max}$ (m)
5	1	0.2	2.87	0.475	6.934	65.98
5	1	0.5	5.71	0.645	6.910	121.54
5	1	1.0	9.60	0.812	6.886	192.93
5	10	0.2	5.11	0.220	6.969	142.15
5	10	0.5	10.15	0.299	6.958	261.85
5	10	1.0	17.08	0.377	6.947	415.65
3	1	0.2	2.87	0.401	5.350	60.60
3	1	0.5	5.71	0.544	5.324	111.62
3	1	1.0	9.60	0.685	5.298	177.19
3	10	0.2	5.11	0.186	5.388	130.55
3	10	0.5	10.15	0.252	5.376	240.48
3	10	1.0	17.08	0.318	5.365	381.73

TABLE 2. Values for a_{min} and corresponding wave characteristics.

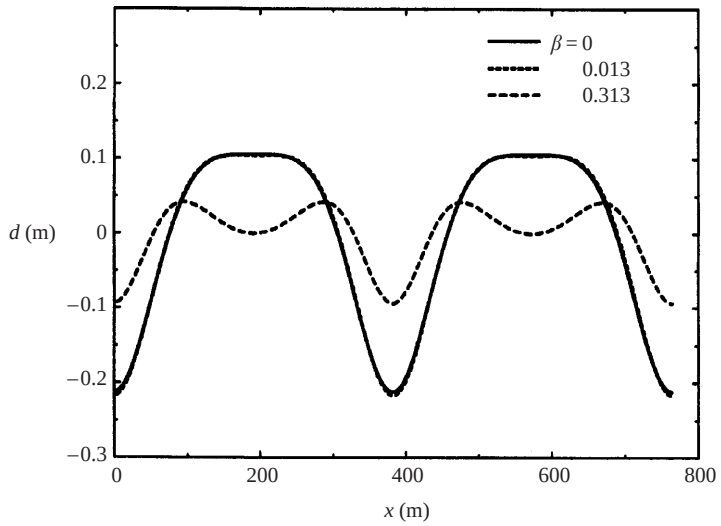

FIGURE 2. Nonlinear wave profiles.

The maximum bending stress produced by the propagating waves can be obtained from (15) for the simplified case as

$$S_{max} = \frac{E}{1-\nu^2}\frac{\eta}{l^2}\frac{a^{3/2}}{\sqrt{35d_o}}. \tag{22}$$

For an ice cover with a maximum flexural strength S_b, the minimum wave amplitude that can cause ice cover fracture is

$$a_{min} = \left(\frac{S_b(1-\nu^2)}{E\eta} l^2\sqrt{35d_o}\right)^{2/3}. \tag{23}$$

Equations (16), (17) and (23) can be used to determine a_{min} and corresponding values of U and L_w, which is the maximum wavelength corresponding to a_{min}. Table 2 gives sample values for different ice cover conditions with $S_b = 0.6$ Mpa. The ranges of wave amplitude, wave speed and wavelength are consistent with the limited field observations available (Parkinson 1982; Gerard *et al.* 1984; Prowse 1986).

β	L_w (m)	a (m)	b (m)	k	α	g	$U/c-1$
0	381.7	0.3180	0	0.7071	0.1659	0.3333	−0.0106
0.013	387.5	0.3230	0.0186	0.7162	0.1645	0.3056	−0.0120
0.113	414.9	0.4310	0.1836	0.7827	0.1617	0.1309	−0.0237
0.213	440.8	0.5300	0.3598	0.8325	0.1601	0.0162	−0.0349
0.313	442.4	0.5787	0.4793	0.8432	0.1616	−0.0478	−0.0504

TABLE 3. Solutions of the complete equation for breakup ice cover.

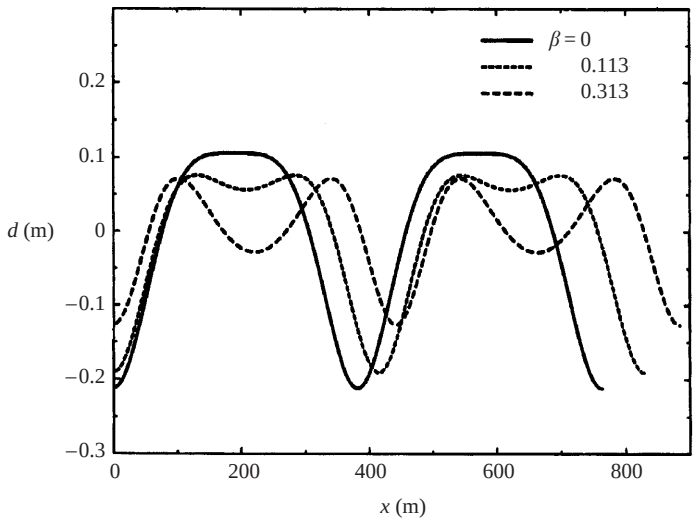

FIGURE 3. Examples of wave profiles that can fracture the ice cover.

For the solution of the complete equation, the maximum bending stress S_{max} in the ice cover can be obtained from (18) as

$$S_{max} = \frac{E}{1-\nu^2}\frac{\eta}{l^2}G_{max}(\kappa), \tag{24}$$

where $G_{max}(\kappa)$ is the maximum value of $G(x,\kappa)$ in the x-coordinate, and

$$G(x,\kappa) = \frac{\alpha^2}{2}\left[20a\kappa^2\,\mathrm{cn}^6\left(\alpha\frac{x}{l},\kappa\right) + (16a(1-2\kappa^2) - 6b\kappa^2)\,\mathrm{cn}^4\left(\alpha\frac{x}{l},\kappa\right)\right.$$
$$\left. + (12a(\kappa^2-1) + 4b(2\kappa^2-1))\,\mathrm{cn}^2\left(\alpha\frac{x}{l},\kappa\right) + 2b(1-\kappa^2)\right]. \tag{25}$$

The maximum value of $G(x,\kappa)$ is difficult to obtain explicitly. It can be obtained numerically by varying the value of x over one wavelength. If the value of S_{max} is found to be larger than the maximum flexural strength S_b, then the ice cover will fracture. The longest wavelength, $(L_w)_{max}$, that will cause fracture can be then determined from (21).

Using the parameters of the last case in table 2, with $F_r = 0.3$, wave conditions that can cause the cover to fracture are shown in table 3. The profiles of these waves are shown in figure 3. This figure shows that if the axial force is large enough, it can

change the shape of the wave. Furthermore, the wave height required to cause the ice cover to fracture is also reduced.

4. Summary

A nonlinear analysis was carried out on the interaction of shallow water waves with a floating ice cover in a uniform channel, and the fracture of the cover under the influence of the wave. The analysis shows that a weakly nonlinear wave equation is a fifth-order Korteweg–de Vries (KdV) equation. The nonlinear wave solutions in the form of cnoidal waves are obtained. The explicit solution for a simplified form of the equation, which neglects the effects of ice cover inertia and axial force, shows that the celerity of the wave is slightly reduced by the existence of the cover. The minimum waveheight that is required to fracture the ice cover is typically in the range of 0.2 to 0.8 m, depending on the cover thickness and strength. The corresponding wavelength, i.e. the distance between the transverse cracks that were generated by the propagating waves varies from 50 to 400 m. For a typical ice cover condition during the spring breakup period, the range is in the order of 50 to 150 m. These results are consistent with the limited field observations. The solution of the complete equation showed that the ice cover inertia effect is negligible. However, a large axial force acting along the ice cover could reduce the wave height that is required to fracture the cover.

This study was partially supported by the US Army Research Office through Grant No. DAAG55-98-1-0520, and the US Army Cold Regions Research and Engineering Laboratory through Contract No. DACA89-94-K-0017.

REFERENCES

Beltaos, S. 1990 Fracture and breakup of river ice cover. *Can. J. Civ. Engng* **17**, 173–183.

Daly, S. F. 1993 Wave propagation in ice-covered channel. *J. Hydraulic Engng* **119**, 895–910.

Daly, S. F. 1995 Fracture of river ice covers by river waves. *J. Cold Regions Engng* **9**, 41–52.

Debnath, L. 1994 *Nonlinear Water Waves*. Academic.

Gerard, R., Kent, T. D., Janowicz, R. & Lyons, R. O. 1984 Ice regime reconnaissance, Yukon River, Yukon. *Cold Regions Engng Specialty Conf., Edmonton* (ed. D. M. Smith), pp. 1059–1073. CSCE.

Grimshaw, R. & Joshi, N. 1995 Weakly nonlocal solitary waves in a singularly perturbed Korteweg-De Vries equation. *SIAM J. Appl. Maths* **55**, 124.

Hunter, J. K. & Scheurle, J. 1988 Existence of perturbed solitary wave solutions to a model equation for water waves. *Physica* D **32**, 253–268.

Karpman, V. I. 1998 Radiation by weakly shallow-water due to higher-order dispersion. *Phys. Rev.* E **58**, 5070.

Mei, C. C. 1983 *The Applied Dynamics of Ocean Surface Waves*. Wiley.

Parkinson, F. E. 1982 Water temperature observations during breakup on the Liard-Mackenzie River system. *Proc. Workshop on Hydraulic of Ice-Covered-Rivers, Edmonton* (ed. D. D. Andres & R. Gerard), pp. 261–290. National Research Council of Canada.

Prowse, T. D. 1986 Ice jam characteristics, Liard-Mackenzie River confluence. *Can. J. Civil Engng* **13**, 653–665.

Prowse, T. D. & Demuth, M. N. 1989 Failure modes observed during river ice breakup. *Proc. 46th Eastern Snow Conf., Quebec City* (ed. J. P. Dempsey & H. H. Shen), pp. 237–241.

Shen, H. T. & Chiang, L. A. 1984 Simulation of growth and decay of river ice cover. *J. Hydraul Engng ASCE* **110**, 958–971.

Shen, H. T., Liu, L. & Chen, Y.-C. 2001 River ice dynamics and ice jam modeling. *Scaling Laws in Ice Mechanics and Ice Dynamics, Proc. IUTAM Symp.*, pp. 349–362. Kluwer.

Shen, H. T., Su, J. & Liu, L. 2000 SPH simulation of river ice dynamics. *J. Comput. Phys.* **165**, 752–771.

Shulyakovskii, L. G. 1972 On a model of breakup process. *Soviet Hydrology, Selected Papers* **1**, 21–27.

Squire, V. A., Dugan, J., Wadhams, P., Liu, A. & Rottier, P. 1995 Of ocean waves and sea ice. *Annu. Rev. Fluid Mech.* **27**, 115–168.

Wadhams, P. 2000 *Ice in the Ocean.* Gordon and Breach.